Biochemical and Biophysical Research Communications **254,** 54–64 (1999)
Article ID bbrc.1998.9801, available online at http://www.idealibrary.com on IDEAL®

The T0 Domain of Rabbit KV1.3 Regulates Steady State Channel Protein Level

Alan S. Segal,*[,1] Xiaoqiang Yao,† and Gary V. Desir‡[,2]
**Department of Medicine, University of Vermont, Burlington, Vermont; †Department of Physiology, Chinese University of Hong Kong, Hong Kong; ‡Department of Internal Medicine, School of Medicine, Yale University, and West Haven VA Medical Center, New Haven, Connecticut*

Received October 27, 1998

The *Shaker* superfamily encodes voltage-gated potassium (Kv) channels. The amino (N) terminus is important for channel assembly and mediates fast inactivation. We recently isolated a Kv channel from rabbit kidney, denoted rabKv1.3 (Yao et al., *J. Clin. Invest.* 97, 2525–2533, 1996) and found that deleting a region (T0 domain, amino acids 3–39) proximal to the T1 recognition domain (a.a 42–185) leads to a 13-fold amplification of Kv current as compared to wild type channels (Yao et al., *BBRC* 249, 492–498). Here we show that deleting the T0 domain affects neither single channel conductance nor channel open probability. Instead, it increases the absolute number of channel proteins present in the membrane. We conclude that the T0 domain is a previously unrecognized *Shaker* Kv1.3, N-terminal regulatory region that modulates steady state channel protein density in the plasma membrane.

Key Words: **ion channel; voltage-gated; *Xenopus* oocyte; patch clamp; cloning; kidney; structure-function; regulatory domain; T0 domain.**

The *Shaker* gene superfamily encodes voltage-gated K (Kv) channels and consists of at least 7 families (Kv1-Kv7) that can be further categorized into subfamilies. For instance, the Kv1 family contains 8 subfamilies, Kv1.1-Kv1.8. All Kv genes cloned to date encode proteins with remarkably similar secondary structures (Fig. 1): intracellular localization of N and C termini, 6 transmembrane segments (S1-S6), a voltage sensor (S4) and a pore (P) region. The S4 segment senses changes in membrane voltage (1-4). Ion permeation occurs via the P region located between the 5th and 6th transmembrane segments (5-8). This is also the region that binds the channel blockers tetraethylammonium (TEA) and charybdotoxin (9,10). Since each Kv subfamily has distinctive kinetic properties, structure-function relationships of Kv proteins have been extensively studied using naturally occurring isoforms and mutants obtained by site-directed mutagenesis. The extreme N terminus mediates fast (type A) inactivation (11,12) in Kv proteins that rapidly inactivate. A more distal N terminal region known as the T1 domain regulates channel assembly (13-15) by serving as a recognition site for heteromultimeric channel assembly within a family, and by preventing co-assembly between families.

Kv1.3 is expressed in brain, lymphocytes, and kidney. In T lymphocytes there are excellent data indicating that the Kv1.3 subfamily mediates the *n* type current (16,17). This current plays an essential role in T-cell proliferation and activation. The *n* type current increases by up to 20 fold when T cells are activated (18-20). Moreover, Kv1.3 channels studied in either *Xenopus* oocytes or in mammalian expression systems demonstrate kinetic and pharmacological properties identical to those of the *n* type current of T lymphocytes. Furthermore, blockers of *n* type current inhibit mitogen-induced cell division and secretion of interleukin 2. Although the molecular structure of Kv1.3 channels is known, the mechanisms by which *n* type current is stimulated in activated lymphocytes remain incompletely understood. However, it is known that the rise in Kv1.3 current that occurs with T cell activation is accompanied by an increase in Kv1.3 protein density at the plasma membrane, despite a decrease in steady state mRNA level (17).

[1] Support for this research was provided by Physician-Scientist Award (NIH DK-02103).
[2] Support was also provided by the Veterans Administration (Career Development and Merit Review Awards), NIH (DK48105B), and Established Investigator AHA.

Address correspondence and reprint requests to: Gary Desir M.D., Yale University School of Medicine, 2073 LMP, 333 Cedar Street, New Haven CT 06510. Fax: (203) 937-4723. E-mail: gary.desir@yale.edu.

0006-291X/99 $30.00

We have previously proposed that in the kidney, rabKv1.3 may be involved in K^+ reabsorption in the inner medullary collecting duct, and its expression in the membrane may be modulated by the composition of the luminal fluid (21). As discussed in the paper, this hypothesis is based on functional data from the papillary cell line GRBPAP1 and from RNA expression data in rabbit kidney. To our knowledge there isn't yet functional evidence for Kv channels in native kidneys.

We recently identified a region at the N terminus of Shaker KV1.3, (T0 regulatory domain, amino acids 3-39 rabbit KV1.3) which modulates channel expression. Deletion of the entire region increases whole cell current by more than 10 fold (22). Site-directed mutagenesis studies indicate that negatively charged amino acids are essential components of the T0 domain. Furthermore, gain-of-function mutations do not affect clathrin-mediated endocytosis.

In the present study, we examined the molecular mechanisms underlying the gain-of-function mutations in the T0 domain, and find the observed increase in Kv1.3 current to be caused largely by a dramatic increase in Kv1.3 protein at the plasma membrane.

MATERIALS AND METHODS

Generation of mutant channels. The amino acid (a.a.) sequence for the N terminus of rabKv1.3 (Genbank accession # U38240) shares significant similarity to its homologues in human, mouse, and rat (21). The polymerase chain reaction (PCR) was employed to create a series of deletion mutants at the amino terminus of rabbit Kv1.3 (rabKv1.3) (Fig. 1). The NT3-12, NT3-28 deletion mutants produced currents indistinguishable from wild type, and these clones were not studied further. The NT3-39 mutant was generated by deleting the DNA sequence coding for a.a. 3-39 from wild type rabKV1.3 DNA using PCR. The sense primer (GGATCCTAATACGACTCACTATAGGGAGGAGCCACCATGACGGAGCAGGAGTGCTGCGGGGAG) contained a T7 polymerase site and the coding sequence for a.a. 1-2 and 40-51. The antisense primer (TTTTTTTTTCCTGTCCTTGATGGATGGTCT) contained a stop codon and a polyA tail. NT3-39 was amplified by PCR using an Air Thermo Cycler 1605 (Idaho Technologies). The amplified product was cloned into *pBluescript* and sequenced by the method of Sanger (23) to confirm that no other mutations besides the 3-39 deletion were introduced during the amplification process.

Expression in Xenopus oocytes. Stage V-VI *Xenopus laevis* oocytes were dissected from ovarian lobes and stored in modified Barth's solution. Oocytes were injected with 50 nl containing either 5 ng of in vitro-transcribed, 5′-capped rabKv1.3 RNA, 5 ng NT3-39 RNA, or water as a negative control. Whole cell currents were recorded using a standard two-microelectrode voltage clamp (OC-725, Warner Inst.) 1-3 days after injection. Oocytes were impaled with microelectrodes filled with 0.5 M KCl (resistance 0.5-5 MΩ). The bath contained (in mM): 88 NaCl, 2 KCl, 1 $CaCl_2$, 1 $MgCl_2$, 2.5 NaH_2CO_3, 5 HEPES, pH 7.4. Amplified currents were filtered at 2 kHz then recorded and analyzed using PULSE (HEKA Lambretch, F.R.G.) and Igor-Pro (Wavemetrics).

For ensemble currents, the kinetics of activation and inactivation of wild type and NT3-39 mutants were examined as previously described (21). Briefly, current traces were elicited by a single-step command voltage protocol (voltage steps from −80 to +80 mV from a holding potential of −80 mV). Activation parameters (fit of current traces elicited by voltages ranging from −10 to +80 mV) and inactivation parameters (fit of current traces that inactivated, voltage steps from +10 to +80 mV) were determined using the Pulse-Fit program (HEKA). The observed currents were fitted to the Hodgkin-Huxley equation according to a *Simplex* optimization algorithm. The best fit, judged by visual inspection and by examination of the root mean square deviation between fit and data (RMS), was obtained when the number of activation (m) and inactivation gates (h) was set at 1 and 2, respectively. The time constants of activation (τ_{act}) and inactivation (τ_{inact}) were determined from the fit and plotted against voltage.

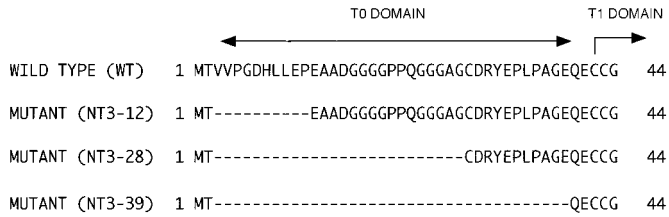

FIG. 1. T0 domain mutations. Amino acids 1-44 of wild type rabKv1.3 and the various deletion mutations that were made. The single letter amino acid (a.a.) code is: A, Ala; C, Cys; D, Asp; E, Glu; F, Phe; G, Gly; H, His; I, Ile; K, Lys; L, Leu; M, Met; N, Asn, P, Pro; Q, Gln; R, Arg; S, Ser; T, Thr; V, Val; W, Trp; Y, Tyr. The T1 domain mediates subunit interaction.

Whole-cell K conductance for each test potential was determined with the oocyte in the high K bath (i.e., $E_K \sim 0$ mV). After holding at −80 mV for a long enough time to allow complete removal of inactivation, a 50 ms pulse to the test potential to activate the channels was followed by a post-pulse to −100 mV. After leak subtraction, the whole-cell K conductance (G_K) at the test potential was calculated as the tail current (at −100 mV) divided by −100 mV. That is,

$$G_K(\mu S) = \frac{I_{tailat-100mV}\mu A}{-0.1V}$$

Normalized current (G_K/G_Kmax) was then plotted against voltage.

Single channel currents were amplified with a List EPC-7 patch clamp amplifier (List Electronics, Darmstadt, Germany). Currents were filtered at 1 kHz (8 pole Bessel) and sampled at 2500 s^{-1}. Records were analyzed using software written in our laboratory (24). The patch pipette (Corning 7052, 2-4 MΩ) contained (in mM): 88 NaCl, 2 KCl, 1 $CaCl_2$, 1 $MgCl_2$, 2.5 NaH_2CO_3, 5 HEPES, pH 7.4. The bath contained (in mM): 88 KCl, 2 NaCl, 1 $CaCl_2$, 1 $MgCl_2$, 2.5 NaH_2CO_3, 5 HEPES, pH 7.4. Voltage was stepped from a holding potential of −80 mV to the command potential indicated.

Detection of channel expression by immunofluorescence. The primary antibody used in these studies has been previously characterized (25). It is a rabbit polyclonal raised against the first extracellular domain of human Kv1.3 (hKv1.3) (residues 198-242). This region is 94% identical to that of rabKv1.3. Pre-immune serum was also available.

Oocytes were injected with either water, 5 ng RNA from wild type or 5 ng NT3-39. Peak current for each oocyte was measured as described above. The oocyte was then placed in a hypertonic solution consisting of 200 mM potassium aspartate, 20 mM KCl, 1 mM $MgCl_2$, 5 mM EGTA, 10 mM HEPES, pH 7.4 and the vitelline membrane was mechanically removed. Oocytes were frozen, unfixed, in Tissue-Tek OCT compound (Miles, Elkart, IN) using an isopentane bath in liquid nitrogen and stored at −70°C. Eight micron sections cut using a cryostat were collected on gelatin coated slides. Before use, tissues were fixed in acetone at −20°C for 3 minutes and rehydrated in

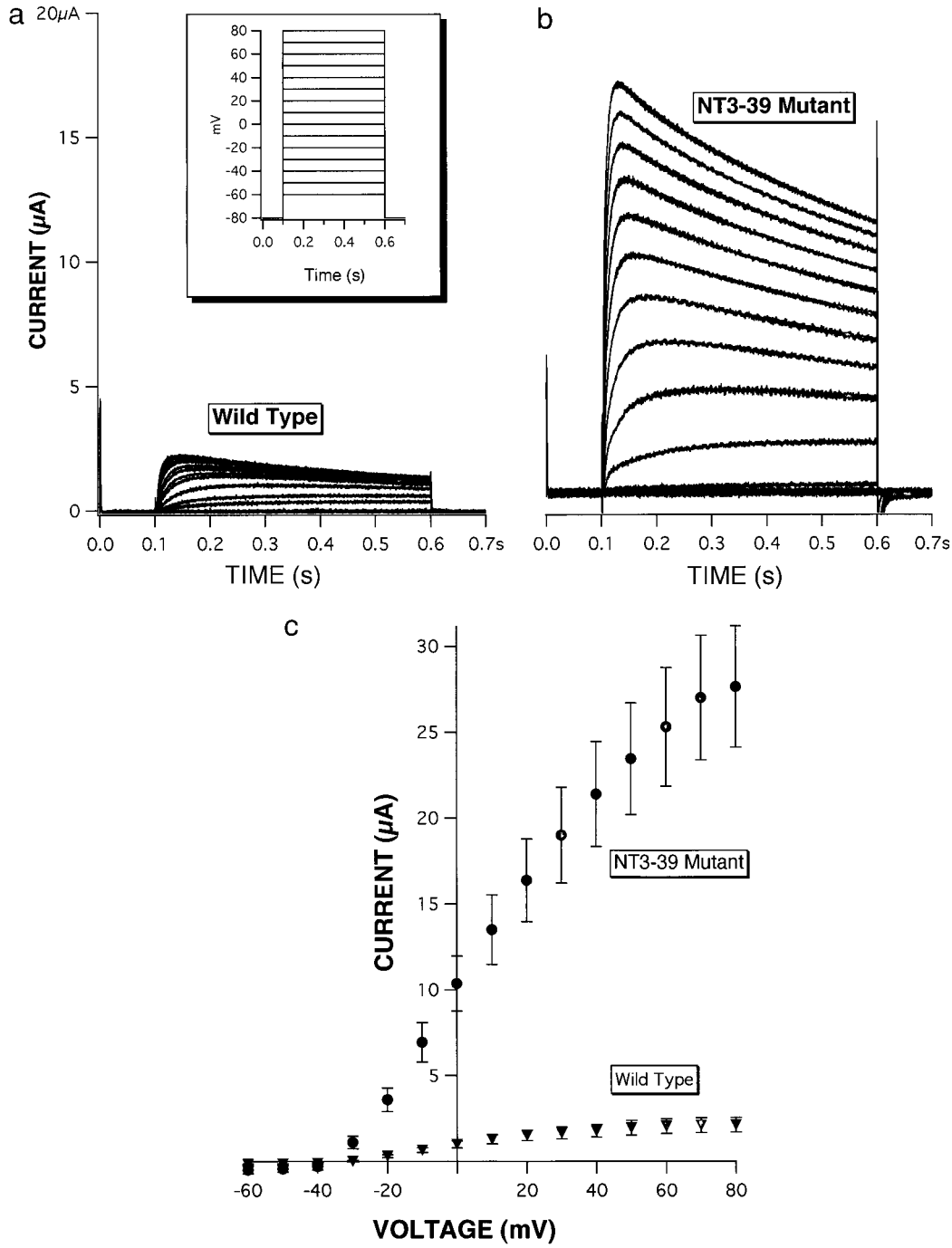

FIG. 2. Gain-of-function does not affect ensemble kinetics or voltage dependence. Representative whole cell currents for (*a*) wild type and (*b*) NT3-39 rabKv1.3 expressed in *Xenopus* oocytes shows the gain-of-function generated by the NT3-39 mutation. Currents were elicited by two-microelectrode voltage clamp using (*inset*) 500 ms pulses from −60 to +80 mV in 10 mV increments from a holding potential −80 mV with a 20 s interpulse interval to allow channels to recover from inactivation. (*c*) Peak current-voltage relationship for wild type (▼) ($n = 19$) and NT3-39 (●) channels ($n = 36$). (*d*) Current traces were elicited for wild type (▼) and NT3-39 mutant channels (●) by a single-step command voltage protocol (voltage steps from −80 to +80 mV in 10 mV increments from a holding potential of −80 mV). Time constants of activation (τ_{act}, *left panel*) were obtained by fitting current traces elicited by voltages ranging from −10 to +80 mV, and those for inactivation (τ_{inact}, *right panel*) were obtained by fitting currents traces that inactivated (voltage steps from +10 to +80 mV), as described in the Materials and Methods.

phosphate buffered saline (PBS) at room temperature. The slides were incubated in PBS containing 0.3% Triton and 0.1% SDS for 15 min at room temperature then washed in PBS and incubated in blocking solution (16% goat serum, 0.3% Triton X-100, 0.43 M NaCl, 20 mM $NaHPO_4$, pH 7.4). The slides were incubated overnight at 4°C with either the primary antibody (1:100 dilution) or the pre-immune

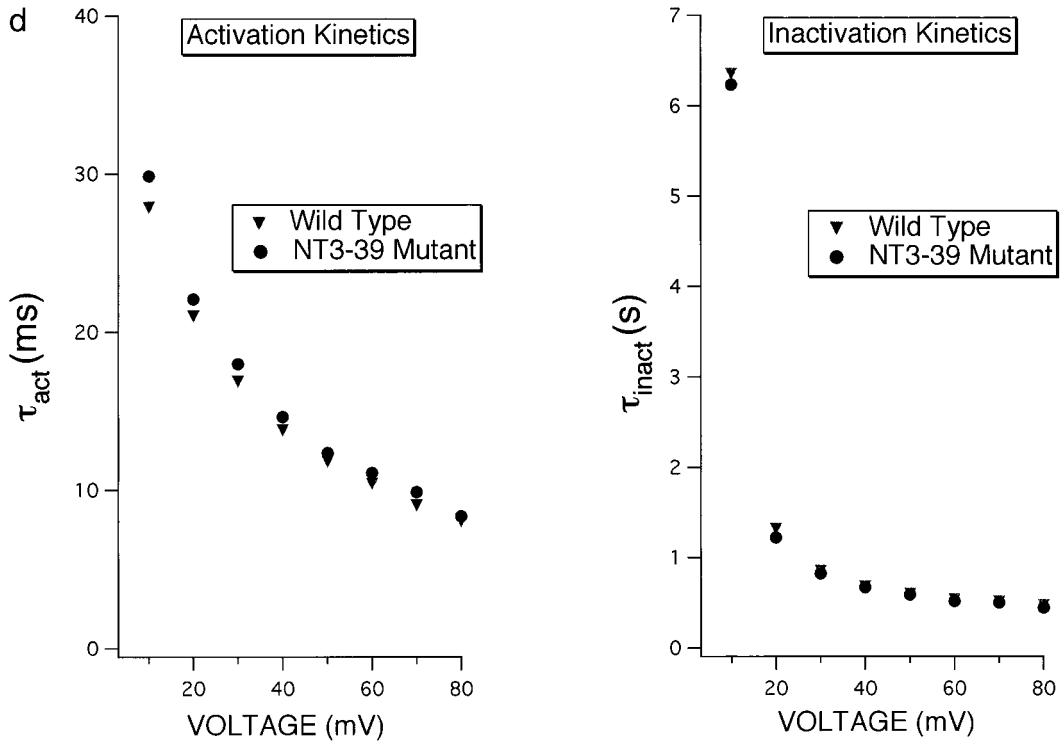

FIG. 2—*Continued*

serum (1:100 dilution). The slides were washed in blocking solution, and then incubated for 1 h at room temperature with a fluorescein isothiocyanate (FITC) labeled goat, anti-rabbit secondary antibody (Zymed Laboratories, South San Francisco, CA), at a dilution of 1:100. Finally, the slides were washed in PBS, and the signal was preserved in crystal/mount (Biomeda, Foster City, CA). Sections were examined within 4 h using a Zeiss fluorescence microscope and photographed at a magnification of 160×.

Fluorescent signals were analyzed using NIH Image software (National Institutes of Health, Bethesda, MD). The entire area corresponding to the plasma membrane was selected and the integrated density (corrected for background) of all pixels was measured. To facilitate comparison, these data were arbitrarily normalized to 50,000 pixels by multiplying each integrated density by 50,000/(# pixels in selected area).

RESULTS AND DISCUSSION

A Deletion Mutation at the Amino Terminus of rabKv1.3 Produces a Gain-of-Function

Rabbit Kv1.3 has a secondary structure and kinetics properties similar to other previously cloned Kv1.3 channels, and the overall sequence identity with human, mouse and rat Kv1.3 channels is 93.8, 90.9, and 91.3%, respectively (21). We initially chose to mutate the N terminus because it regulates tetrameric channel assembly as discussed in the Introduction. The mutations shown in Fig. 1 were generated in rabKv1.3 in order to test if the region (amino acids 1-40) immediately preceding the T1 recognition domain (amino acids 41-185) was important for channel function. We reasoned that these mutations should not interfere with the ability of individual subunits to form either homo- or heterotetramers since the T1 domain remained intact, nor should they affect inactivation properties of the channels, since rabKv1.3, like the other members of the Kv1.3 subfamily, does not undergo fast inactivation.

cRNA of wild type or mutants was injected in *Xenopus* oocytes and channel expression was analyzed using two microelectrode voltage clamp and patch clamp. Deletions of amino acids 3-12, 3-28, caused no detectable changes in whole cell current expression or kinetics: NT3-12 = 2.1 ± 0.2 μA, n = 3, and NT3-28 = 2.0 ± 0.1 μA, n = 3. Therefore, these mutations were not characterized further. In contrast, as shown in Figs. 2a and 2b, deleting amino acids 3-39 (NT3-39 mutant) results in a 13-fold increase in whole cell current 3 days post injection. The current-voltage (I-V) plot for the peak currents is shown in Fig. 2c. Peak current at +80 mV was 2.13 ± 0.42 μA for wild type (n = 19) as compared to 27.7 ± 3.5 μA (n = 36) for NT3-39 mutant ($p < 0.0001$). The difference in whole cell current between wild type and NT3-39 mutant was even more dramatic 24 hours post injection. Indeed, Kv1.3 current was never detected in oocytes within 24 hours of injection with wild type RNA ($n > 50$), while oocytes

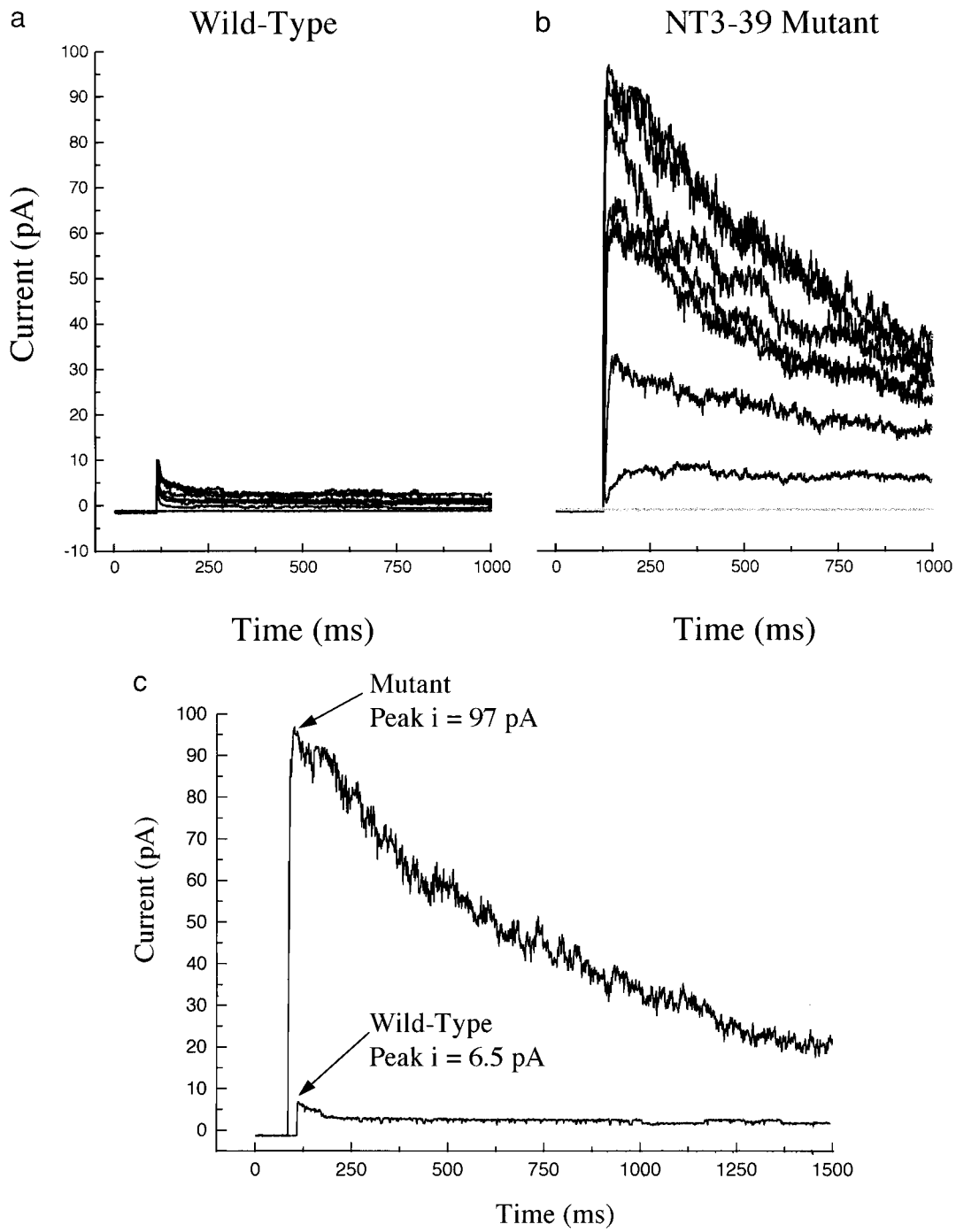

FIG. 3. Gain-of-function is recapitulated in membrane patches. Ensemble currents from cell-attached membrane patches made on oocytes injected either with cRNA for (*a*) wild-type or (*b*) NT3-39 rabKv1.3 channels. Currents were elicited by stepping to test potentials ranging from −60 mV to +80 mV from a holding potential of −80 mV. Between steps, the potential was held at −80 mV for at least 60 s to allow channels to recover from inactivation. (*c*) Comparison of the current transient upon stepping to +60 mV shows a nearly 15-fold amplification of ensemble current in the NT3-39 mutant relative to wild-type. Oocytes were bathed in high KCl solution and patch pipettes were filled with low KCl solution, as described in Materials and Methods.

expressing the NT3-39 mutant had whole cell currents of 17.7 ± 2 μA (n = 20). Current measured 3 days post injection in both wild type and mutant correlated directly with the amount of cRNA injected, up to a maximum of 10 ng. We were unable to evaluate the effect of larger amount of cRNA on current expression since

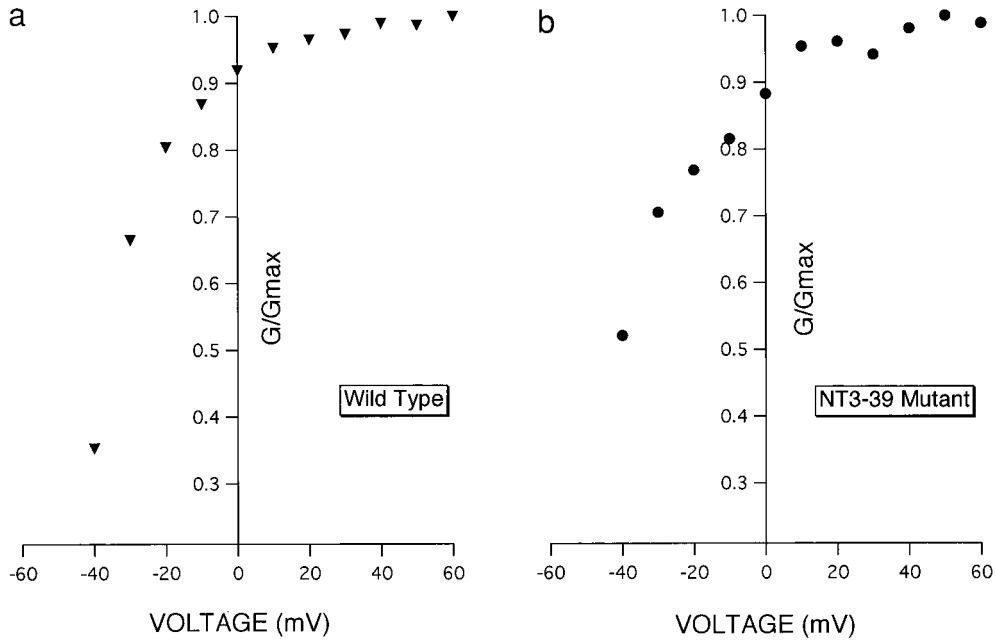

FIG. 4. Mutation does not significantly affect the voltage dependence of the ensemble conductance. Ensemble conductance/Maximal conductance-voltage (G/Gmax-V) relations for (*a*) wild-type ($n = 3$) and (*b*) NT3-39 ($n = 3$) rabKv1.3 obtained as described in Materials and Methods. Similar G/Gmax-V relations indicate that the deletion mutation does not alter the voltage dependence of the ensemble conductance.

oocytes injected with 15 ng NT3-39 cRNA often had currents exceeding the capacity of the voltage clamp (100 μA).

These data confirm our previous findings (22). Others have reported that deletions at the N terminus of Kv1.3 channels caused a decrease in whole cell current (26). These results could be explained by the fact that the deletion examined in that study included a portion of the T1 domain.

Since whole cell conductance (G) is given by,

$$G = P_o \cdot g \cdot N$$

several mechanisms could underlie the gain of function observed in the NT3-39 mutant: an increase in 1) channel open probability (Po), 2) single channel conductance (g), and/or 3) the number of functional channel proteins (N) expressed. The experiments that follow were designed to test these possibilities.

The Mutation Does Not Significantly Affect the Kinetics of the Ensemble Current

Whole cell current traces obtained for wild type and for NT3-39 mutant channels expressed in *Xenopus* oocytes (see Figs. 2a and 2b) reveals that although the NT3-39 mutation amplifies the magnitude of expressed current, it does not significantly affect the kinetics of activation and inactivation. Indeed, the time constants of activation (τ_{act}) and inactivation (τ_{inact}), determined as described in the Materials and Methods, were nearly identical for wild type and NT3-39 mutants (Fig. 2d), and the same as previously reported for rabKv1.3 (21).

Patch-clamp recordings from oocytes recapitulate the whole-cell findings. Active channels (typically 1 to 4) were observed in only ~10% of membrane patches from oocytes injected with wild-type RNA (Fig. 3a). In contrast, ~80% of membrane patches from oocytes injected with mutant RNA contained numerous active channels (Fig. 3b). Thus, the gain-of-function mutation is reproduced at the level of a membrane patch (Fig. 3c). Peak current is ~15-fold higher in patches containing mutant channels. Channels in the membrane patches also follow inactivation kinetics similar to those seen for the whole-cell (see Fig. 3b). For example, for mutant channels the time constant of inactivation (τ_{inact}) upon depolarizing from −80 mV to +60 mV is about 650 ms measured in whole oocytes, and about 700 ms in membrane patches.

The Mutation Does Not Significantly Affect the Voltage Dependence of the Ensemble Current

The voltage dependence of the ensemble current is similar for wild-type and mutant channels (see Fig. 2c). The activation "threshold" for outward current is between −40 and −30 mV for both wild type and mutant, suggesting that the NT3-39 deletion does not greatly

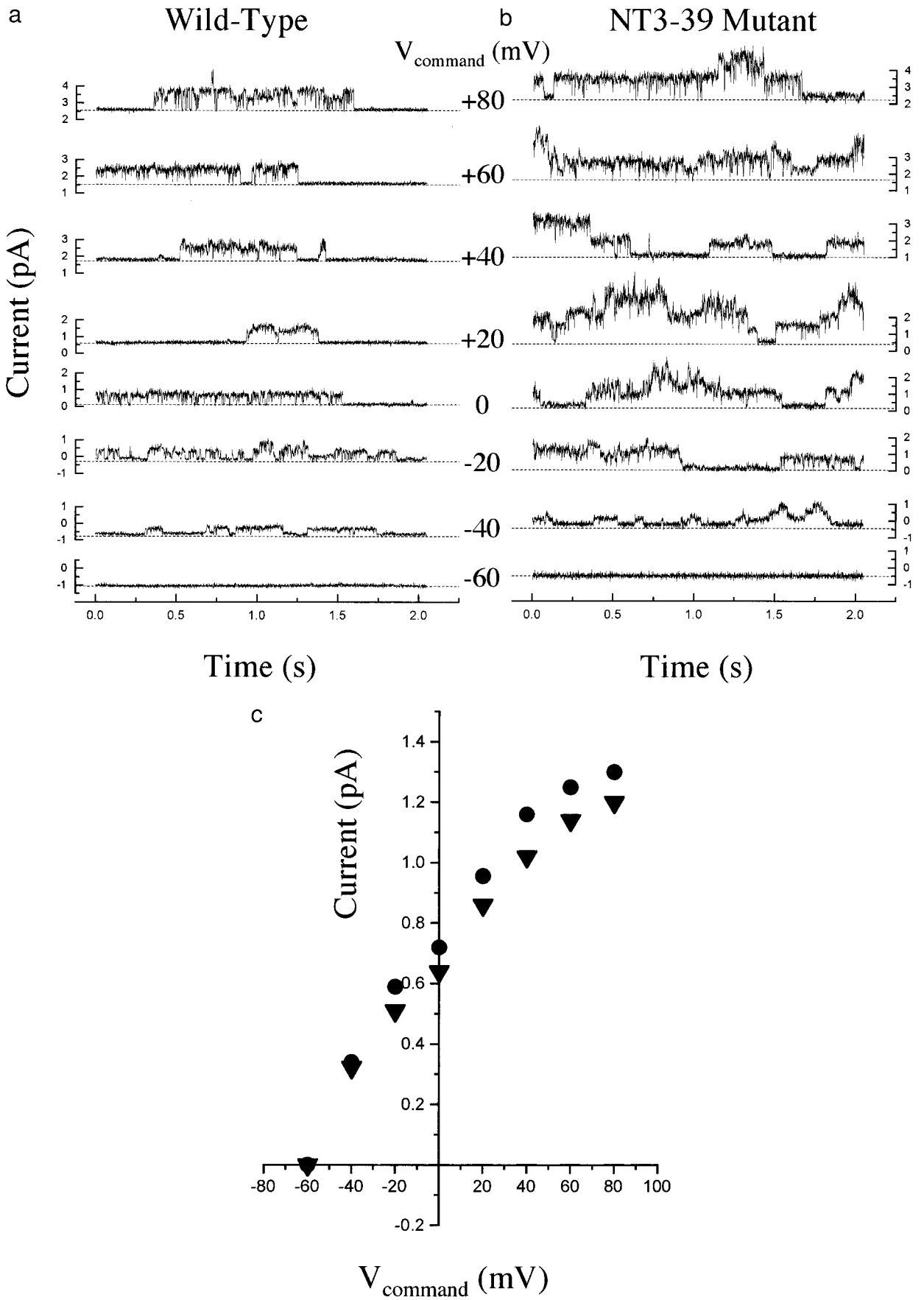
a
Wild-Type
b
NT3-39 Mutant
V command (mV)
+80
+60
+40
+20
0
-20
-40
-60
Current (pA)
Time (s)
Time (s)
c
Current (pA)
V command (mV)

influence the voltage sensor or gate. Moreover, the voltage of half-maximal activation of peak current occurs at about 0 mV for both channels.

To examine the voltage dependence of the ensemble conductance in more detail, G/Gmax-V relations were constructed using the activation pulse/post-pulse tail current protocol outlined in Materials and Methods. Such analysis reveals that the shape of the G/Gmax-V characteristic for the wild-type channel (Fig. 4a) is essentially the same as that for the mutant channel (Fig. 4b), and the voltage at which $G/G_{max} = 0.5$ is about −37 mV for both.

Since both wild-type and mutant channels exhibit inactivation, the "open probability" peaks at the moment of depolarization. Thus, to explain the observed gain-of-function solely on the basis of open probability would require that the P_o of the mutant be 13 times that of the wild-type channel. Given the similar voltage dependence, even if P_o is assumed to be 1 for the mutant, this would imply that the P_o of the wild-type channel does not exceed 0.077 at the moment of depolarization. However, single-channel records of wild-type channels suggest P_o is well above this value just after depolarization (see Fig. 3c and (21)). Indeed, given their similar Boltzmann distributions, it is likely that both channels have the same "open probability" prior to inactivation.

The Gain-of-Function in the Mutant Is Not on the Basis of Single Channel Conductance

The "magnification" of ensemble conductance could be explained, at least in part, if the underlying unitary channel conductance of the mutant was much greater than that of the wild-type. However, patch-clamp recordings of wild-type (Fig. 5a) and mutant (Fig. 5b) single channels establish that the unitary conductance is only slightly increased in the mutant. The I-V relations (Fig. 5c) show that between −40 mV and +40 mV, $g_{\text{wild-type}} = 8.7$ pS and $g_{\text{mutant}} = 10.0$ pS. Such an increase can not explain the 13-fold magnification in whole-cell conductance. Thus, we conclude that the gain-of-function expressed by mutant channels is not primarily on the basis of single-channel conductance.

Taken together, these findings strongly suggest that the NT3-39 deletion mutation does not significantly alter the voltage dependence or single channel conductance.

The Gain-of-Function in the Mutant Is Due to an Increase in Plasma Membrane Channel Protein Density

Since the effects of the NT3-39 deletion mutant on channel behavior and conductance did not appear sufficient to explain the observed "magnification" of whole-cell conductance, we reasoned that the gain-of-function must be primarily due to an increase in channel protein expression on the plasma membrane. We combined electrophysiological methods with immunofluorescence to investigate this possibility. *Xenopus* oocytes were injected with either water or wild type or NT3-39 mutant cRNA, and whole cell current was measured. Subsequently, channel protein density in the plasma membrane of the same oocytes was assessed by immunofluorescence using a $K_{v1.3}$-specific polyclonal antibody as described in the Materials and Methods.

Water injected control oocytes did not express Kv current and the Kv1.3-specific antibody did not label their plasma membrane (Fig. 6). In contrast, the antibody did specifically label the plasma membrane of oocytes injected with wild type cRNA (Fig. 6b) that had expressed Kv1.3 current. Furthermore, in oocytes expressing NT3-39 mutant channels, the immunofluorescence signal in the plasma membrane was dramatically intensified (Fig. 6c).

A summary of the immunofluorescence and electrophysiological results for the three groups of oocytes is shown in Fig. 6d. Water injected oocytes show negligible current (0.16 ± 0.02 μA at +60 mV, n = 6 cells) and minimal fluorescence (22.0 ± 8.7, n = 6 cells) when compared to oocytes injected with wild type Kv1.3 (1.22 ± 0.09 μA at +60 mV and fluorescence: 70.0 ± 24.9, n = 6 cells). However, oocytes injected with mutant Kv1.3 show a seven-fold increase in current (8.5 ± 0.6 μA at +60 mV, n = 6 cells) and exhibit a five-fold increase in fluorescence (341.4 ± 69.5, n = 6 cells) when compared to the wild type. These data strongly suggest that the mutation leads to a marked increase in the density of functional channel proteins (N) in the plasma membrane.

From these data we conclude that the NT3-39 mutation increases whole cell current by up-regulating the density of channel protein in the plasma membrane.

FIG. 5. Gain-of-function in mutant rabKv1.3 is not on the basis of single channel conductance. Steady-state single channel records from cell-attached patches made on *Xenopus* oocytes expressing (*a*) wild-type or (*b*) NT3-39 mutant rabKv1.3 channels show that their unitary conductances are not significantly different. However, the channel density appears to be higher in oocytes expressing the mutant. (*c*) The current-voltage relations are nearly identical. A linear fit between −40 mV and +40 mV yields a conductance of 8.7 pS and 10.0 pS for wild type (▼) and NT3-39 (●), respectively. Oocytes were bathed in high KCl solution and patch pipettes were filled with low KCl solution.

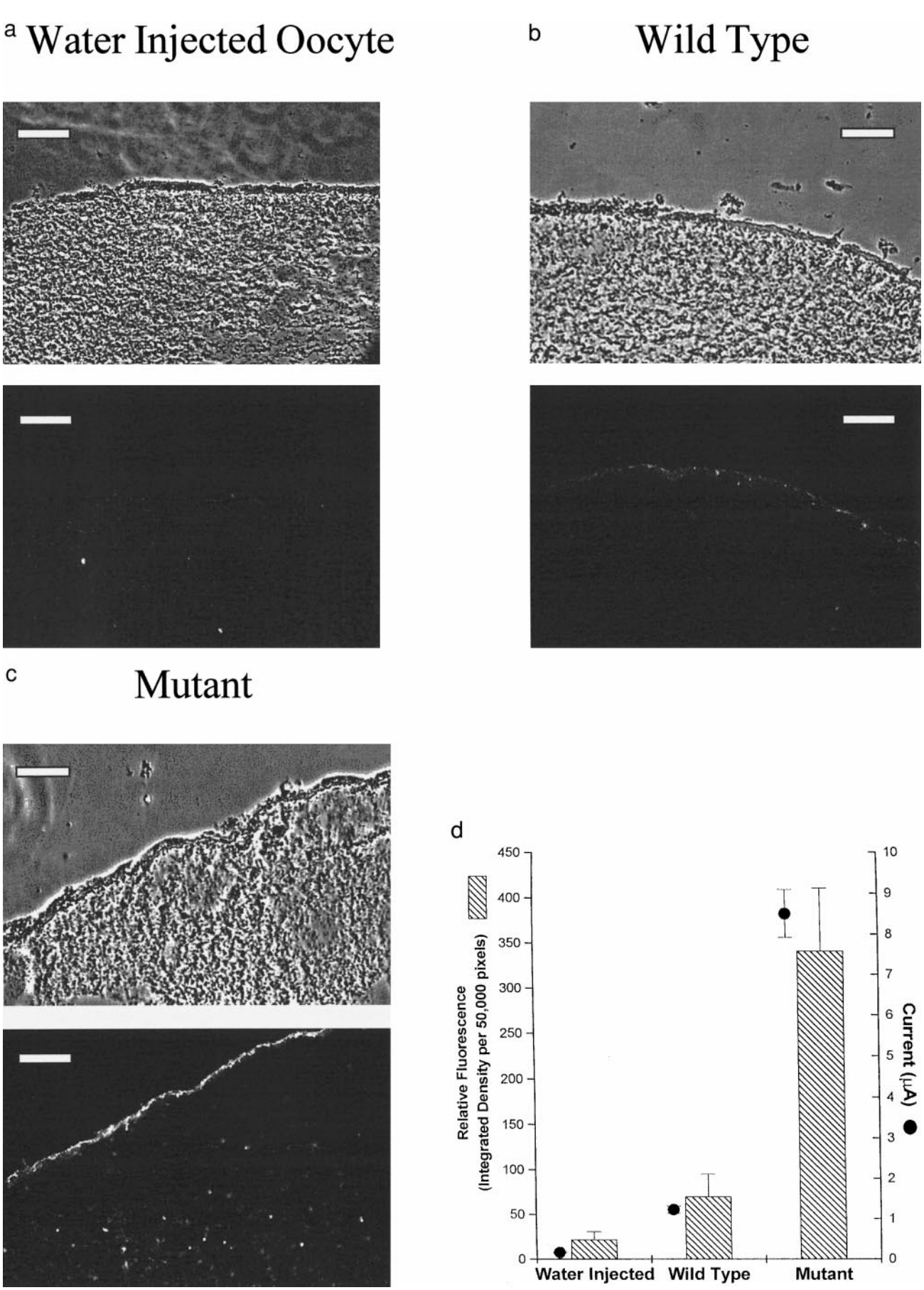
a Water Injected Oocyte
b Wild Type
c Mutant
d
Relative Fluorescence
(Integrated Density per 50,000 pixels)
Current (μA)
0
50
100
150
200
250
300
350
400
450
0
1
2
3
4
5
6
7
8
9
10
Water Injected
Wild Type
Mutant

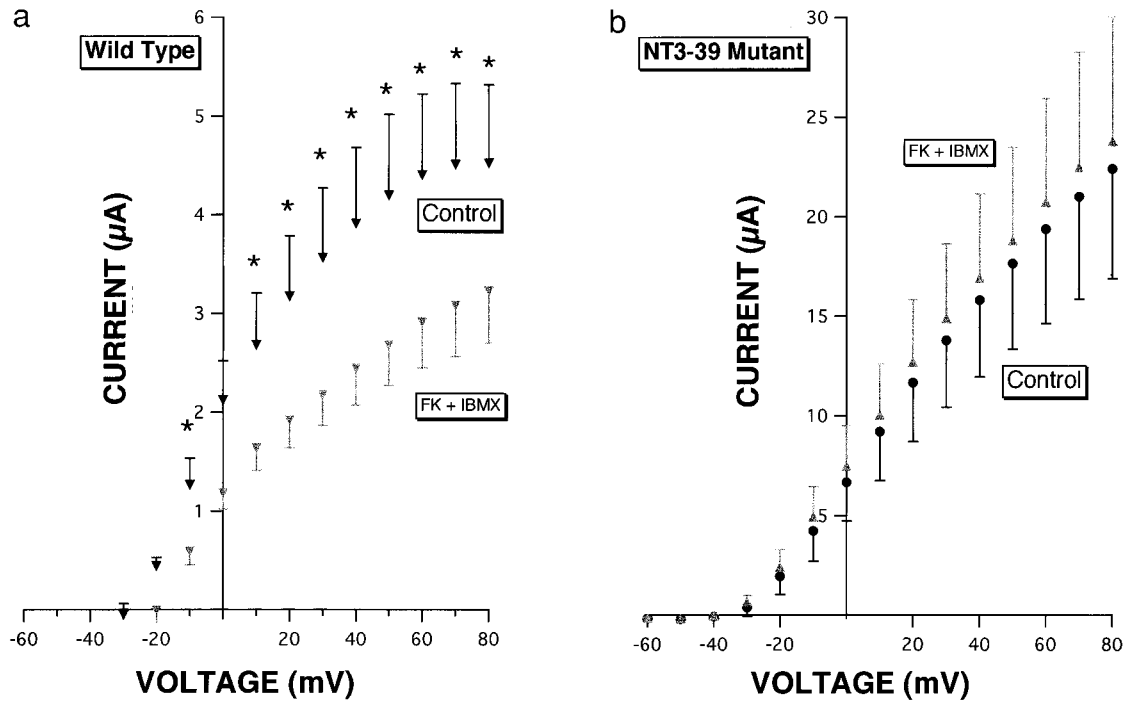

FIG. 7. NT3-39 mutant channels are regulated differently than wild type channels. Stimulation of the cAMP second messenger pathway (with 10 μM FK plus 1 mM IBMX) has an inhibitory effect on (*a*) wild type channels ($n = 3$), but tends to activate (*b*) NT3-39 mutant channels ($n = 3$). *Xenopus* oocytes were injected with either 5 ng of wild type or NT3-39 mutant RNA. Peak current-voltage relationships are shown before and after the addition the indicated compounds. Currents were elicited by two-microelectrode voltage clamp using 500 ms pulses from −60 to +80 mV in 10 mV increments from a holding potential −80 mV with a 20 s interpulse interval to allow the channel to recover from inactivation.

Effect of Cytochalasin D, PKA, and PKC on Channel Activity

Cytochalasin D: It is possible that, *in vivo,* Kv1.3 channel protein density in the membrane is dynamically regulated by intracellular signals that modulate the phosphorylation state of the N terminus or its interaction with either the cytoskeleton or with as yet unknown intracellular proteins. Since it is reasonable to hypothesize that such a signal(s) would regulate wild type and mutant channel activity differently, we tested the effect of disrupting the actin cytoskeleton with cytochalasin D (5 μM). The data show that both wild type (98.2 ± 1%, at +80 mV, n = 4) and NT3-39 mutant channels (98.1 ± 1%, at +80 mV, n = 4) were inhibited.

We also tested the effect of phosphorylation by protein kinase C (PKC) and protein kinase A (PKA) on whole cell currents of oocytes injected with either wild type or NT3-39 mutant RNA.

PKC: Stimulation of endogenous PKC by 10 nM PMA (phorbol 12-myristate 13-acetate) led to a similar decrease in whole cell current of oocytes injected with either wild type (94.6 ± 1%, at +80 mV, n = 4) or NT3-39 RNA (93 ± 2%, at +80 mV, n = 4). In contrast, 4α-phorbol-12,13-didecanoate (10 nM, an inactive analogue of PMA), had no significant effect on currents in oocytes injected with either wild type (decreased by 9.5 ± 4.9%, n = 4) or NT3-39 RNA (decreased by 1.7 ± 1.7%, n = 4).

PKA: In contrast to PKC, stimulation of endogenous PKA activity by 10 μM forskolin and 1 mM IBMX

FIG. 6. Gain-in-function is due to an increase in channel protein density. Wild-type and NT3-39 mutant rabKv1.3 channel protein expression in *Xenopus* oocytes was detected by immunofluorescence using a Kv1.3-specific primary antibody and a FITC-labeled secondary as described in the Materials and Methods. Incubation with preimmune serum resulted in no detectable labeling of water injected control, wild type or NT3-39 RNA injected oocytes (not shown). Representative results obtained with immune serum are shown, and peak currents measured at $V_{command} = +60$ mV for each individual oocyte are also indicated. The scale bar in each panel represents 50 μm. (*a*) Control oocytes injected with 50 nl water yielded minimal voltage-gated current (0.16 ± 0.02 μA) and fluorescence ($n = 6$ cells). (*b*) Oocytes injected with 5 ng wild type RNA; peak current of 1.22 ± 0.09 μA ($n = 6$ cells). (*c*) Oocytes injected with 5 ng NT3-39 RNA; peak current 8.5 ± 0.6 μA ($n = 6$ cells). (*d*) Summary of immunofluorescence and current data for three groups of oocytes. Oocytes injected with the mutant expressed significantly more fluorescence (341.4 ± 69.5 vs. 70 ± 24.9, $p < 0.005$, n = 6 cells) and current (8.5 ± 0.6 μA vs. 1.22 ± 0.09 μA, $p < 10^{-6}$, n = 6 cells) than those injected with wild type Kv1.3.

(3-isobutyl-1-methylxanthine) decreased whole cell current of oocytes expressing wild type channels (Fig. 7a), but had no significant effect on oocytes expressing NT3-39 mutant channels (Fig. 7b). In contrast, an inactive analog of forskolin (1,9 dideoxy-forskolin, 10 μM) had no significant effect on currents in oocytes injected with either wild type (decreased by 3.3 $\pm$ 4.3%, n = 4) or NT3-39 RNA (decreased by 6.3 $\pm$ 7.9%, n = 4).

These data suggest, unlike NT3-39 mutant, wild type Kv1.3 channel activity is down regulated because of channel phosphorylation or interaction of a phosphorylated protein with the channel. The gain-of-function in NT3-39 mutant could be partly due to the lack of constitutive inhibition by PKA, in which case one would expect PKA inhibitors to increase wild type channel current and to have no effect on NT3-39 channels. That appears to be the case since wild type Kv1.3 current increases by 25 $\pm$ 3.1% in oocytes incubated for 20 min membrane permeant PKA inhibitors (H-8 5 μM, n = 3 and H-89 200 μM, n = 3), while NT3-39 current remains unchanged. However, since the magnitude of the effect of PKA-dependent phosphorylation processes on wild type channel activity is small, we conclude that they play a minor role in the gain-of-function of the NT3-39 mutant.

CONCLUSION

We have discovered a region, T0 domain, at the N terminus of rabKv1.3 (a.a. 3-39) that appears to regulate steady state channel protein density in the plasma membrane. Compared to wild type, deleting the T0 domain leads to a 13-fold amplification of whole cell Kv current, at least in part by increasing the absolute number of channel proteins present in the membrane but without affecting single channel conductance. It is important to note that a small increase in the open probability of mutant channels can not be excluded. This deletion does not affect inhibition of channel activity by PKC, but attenuates inhibition by PKA. We previoulsy excluded a role for clathrin-mediated endocytosis. but did not examine non-clathrin mediated endocytosis or changes in the rates of insertion. Further studies are necessary to establish the precise mechanism(s) by which deletions in the N terminus result in higher steady state channel density in the membrane.

Our findings suggest that functional modulation of the N terminus of Kv1.3 may in part underlie the increase in *n* type current that occurs when T lymphocytes become activated. In renal epithelia, rabKv1.3 may be involved in K^+ reabsorption in the inner medullary collecting duct (IMCD). We have proposed that rabKv1.3 is localized to the basolateral membrane (BLM) of IMCD cells where it allows K^+ exit and recycling under conditions when the ATP-sensitive K^+ (K_{ATP}) channels in the BLM are closed (21). By affecting trafficking and/or lifetime of Kv1.3 in the membrane, the N terminus of Kv1.3 may influence the relative balance between Kv channels and K_{ATP} channels in the BLM.

ACKNOWLEDGMENT

The anti-Kv1.3 antibody was a generous gift of Dr. Mike Cavanaugh.

REFERENCES

1. Bezanilla, K., Perozo, E., Papazian, D. M., and Stefani, E. (1991) *Science* **254,** 679–683.
2. Liman, E. R., Hess, P., Weaver, F., and Koren, G. (1991) *Nature* **353,** 752–756.
3. McCormack, K., Tanouye, M. A., Iverson, L. E., Lin, J. W., Ramaswami, M., McCormack, T., Campanelli, J. T., Mathew, M. K., and Rudy, B. (1991) *Proc. Natl. Acad. Sci.* **88,** 2931–2935.
4. Papazian, D. M., Timpe, L. C., Jan, Y. N., and Jan, L. Y. (1991) *Nature* **349,** 305–310.
5. Pongs, O. (1992) *Trends Pharmacol. Sci.* **13,** 359–365.
6. Heginbotham, L., Abramson, T., and MacKinnon, R. (1992) *Science* **258,** 1152–1155.
7. Hartmann, H. A., Kirsch, G. E., Drewe, J. A., Taglialatela, M., Joho, R. H., and Brown, A. M. (1991) *Science* **251,** 942–945.
8. Yool, A. J., and Schwarz, T. L. (1991) *Nature* **349,** 700–704.
9. MacKinnon, R., and Miller, C. (1989) *Science* **245,** 1382–1385.
10. Goldstein, S. A. N., and Miller, C. (1992) *Biophys. J.* **62,** 5–7.
11. Hoshi, T., Zagotta, W. N., and Aldrich, R. W. (1990) *Science* **250,** 533–538.
12. Zagotta, W. N., Hoshi, T., and Aldrich, R. W. (1990) *Science* **250,** 568–571.
13. Hopkins, W. F., Demas, V., and Tempel, B. L. (1994) *J. Neurosci.* **14,** 1385–1393.
14. Lee, T. E., Philipson, L. H., Kuznetsov, A., and Nelson, D. J. (1994) *Biophys. J.* **66,** 667–673.
15. Shen, N. V., and Pfaffinger, P. J. (1995) *Neuron* **14,** 625–633.
16. Grissmer, S., Dethlefs, B., Wasmuth, J. J., Goldin, A. L., Gutman, G. A., Cahalan, M. D., and Chandy, K. G. (1990) *Proc. Natl. Acad. Sci. U.S.A.* **87,** 9411–9415.
17. Cai, Y.-C., Osborne, P. B., North, R. A., Dooley, D. C., and Douglass, J. (1992) *DNA Cell Biol.* **11,** 163–172.
18. Lewis, R. S., and Cahalan, M. D. (1990) *Annu. Rev. Physiol.* **52,** 415–430.
19. Lee, S. C., Levy, D. I., and Deutsch, C. (1992) *J. Gen. Physiol.* **99,** 771–793.
20. Lewis, R. S., and Cahalan, M. D. (1995) *Annu. Rev. Immunol.* **13,** 623–653.
21. Yao, X., Chang, A. Y., Boulpaep, E., Segal, A. S., and Desir, G. V. (1996) *J. Clin. Invest.* **97,** 2525–2533.
22. Yao, X., Huang, Y., Kwan, H-Y., Chan, P., Segal, A. S., and Desir, G. V. (1998) *Biochemical and Biophysical Research Communications* **249,** 492–498.
23. Sanger, F., Nicklen, S., and Coulson, A. R. (1977) *Proc. Natl. Acad. Sci. U.S.A.* **74,** 560–564.
24. Ahmad, I., Korbmacher, C., Segal, A. S., Cheung, P., Boulpaep, E. L., and Barnstable, C. J. (1992) *Proc. Natl. Acad. Sci. USA* **89,** 10262–10266.
25. Cai, Yun-Cai, and Douglass, J. (1993) *Journal of Biological. Chemistry* **268,** 23720–23727.
26. Aiyar, J., Grissmer, S., and Chandy, K. G. (1993) *Am. J. Physiol. Cell Physiol.* **265,** C1571–C1578.